Research Article

Sciences of Phytochemistry

Green-synthesized Zinc Oxide Nanoparticles from *Cissus aralioides*: Characterization, and Antimicrobial Potentials

Innocent Chukwujekwu Onunkwo, Mary Olire Edema, Christiana E. Ogwuche, Bamidele H. Akpeji

[The author informations are in the declarations section. This article is published by ETFLIN in Sciences of Phytochemistry, Volume 5, Issue 1, 2026, Page 147-159. DOI: 10.58920/sciphy0501537]

Received: 26 December 2025
Revised: 27 March 2026
Accepted: 29 April 2026
Published: 11 May 2026

Editor: Devi Ratnawati

Keywords: Extract, Cissus aralioides, Nanoparticles, Zinc oxide, Antimicrobial activity, Microbes..

Abstract: Antimicrobial resistance represents a critical global challenge due to microbial enzymes that neutralize antibiotic efficacy, prompting the use of nanotechnology to enhance the therapeutic potential of plant properties. In this study, zinc oxide nanoparticles (ZnONPs) were biosynthesized using a methanol extract of *Cissus aralioides* leaves obtained through Soxhlet extraction. Characterization via UV-vis, FTIR, PXRD, SEM, EDX, and TEM revealed a maximum absorption at 398 nm, a bandgap energy of 3.12 eV, and a hexagonal wurtzite structure with an average particle size of 15.90 ± 2.81 nm. FTIR analysis confirmed essential chemical groups (C-H, C=O, O-H), while SEM and EDX showed rough surfaces with a predominant zinc content of 80.76%. The antimicrobial potential of these ZnONPs was evaluated against *Escherichia coli*, *Staphylococcus aureus*, *Aspergillus fumigatus*, and *Candida albicans* using the agar well diffusion method at concentrations of 100–400 mg/mL. Results demonstrated significant antimicrobial activity, with the highest sensitivity observed against *S. aureus* (24.0 ± 0.01 mm), followed by *C. albicans*, *E. coli*, and *Aspergillus* sp., and an estimated minimum inhibitory concentration of 100–300 mg/mL. Consequently, this research highlights the potential of green-synthesized ZnONPs as a viable alternative for managing pathogenic microorganisms.

Introduction

Pathogenic microbes have continued to pose serious health risks globally. Nanotechnology presents broader areas whereby materials which are manipulated to nanoscale (1-100 nm) show increased functionalities and can be applied to tackle human and environmental problems. Studies on nanoparticles in these areas have continued to increase (1-6).

Metal oxide-based nanoparticles possess physical, biological and chemical characteristics which make them highly considered for research and other applications (7). Zinc oxide (ZnO) nanoparticles are among the most studied metal oxide nanoparticles because of their large band gap energy, antimicrobial activity, and their ability to act as UV radiation shield in lowering the risk of skin disorders (8-9). Many techniques including thermal evaporation, solution combustion, magnetic sputtering, pulsed laser deposition, molecular beam epitaxial, etc., can be used to produce ZnO nanoparticles (10-13). However, the green synthesis or biosynthesis of nanoparticles from medicinal plants has shown to be less harmful, economical, and harmless to the environment when compared to other conventional methods (14-19). Scientists and industrialists are very interested in ZnO nanoparticles made from plant extracts and zinc oxide (ZnO) because of its many uses and characteristics (20-24). Some medicinal plant extracts of *Hibiscus rosa-sinensis* (25), *Euphorbia hirta* (7), *Cinnamomum verum* (26), *Aloe vera* (27), groundnut shell (16), *Lippia adoensis* (28), *Moringa oleifera* (29), *Lycopersicon esculentum* (30) and a few others have demonstrated intriguing antibacterial qualities when utilized in the production of ZnO nanoparticles (26).

In the present study, *Cissus aralioides* leaf extract was considered for the synthesis of ZnO nanoparticles. *C. aralioides* is a medicinal plant that is a member of the *Vitaceae* family. It has a length of around 25 m, with stem mainly fleshy and a roughly 5-m-long woody base. It is medium-sized tendril climber found in coastal and savannah areas bordering forests, as well as in primitive dense, swampy, woody and semi-deciduous forests. *C.*

aralioides is also home in Acacia bushlands, termite's mounds, granite cliffs and wet grasslands (31-32). Tropical Africa is the plant's primary home (31). The plant has shown a lot of medicinal components and benefits. The plant's roots have been used to treat malaria and fever. The plant contains steroids, alkaloids, and other essential constituents (33). Some phytochemicals such as alkaloid, terpenoid, flavonoid, saponin, proteins, reducing sugar, and cardiac glycoside, have been found in the plant's leaf (34-36). The plant has long been utilized by the locals to treat conditions like rheumatism, arthritis, discomfort, and swelling; and additionally, solvent extracts from the stem have shown activity against certain harmful microbes (37). The plant has also demonstrated to possess antioxidant (38-40), and anti-inflammatory properties (41-44). A constituent (Aralioidamide A) isolated from the plant's stem, has demonstrated antimicrobial activity (45).

However, despite the usefulness of this plant, its ZnO nanoparticles have not been studied, especially in the area of their antimicrobial activity as ZnO nanoparticles have shown to have a significant suppression effect on microbes when they come in contact with their restive enzyme (beta-lactamase) at their binding location. Therefore, this work focused on creating ZnO nanoparticles with the plant's leaf extract and evaluating their antimicrobial potentials, due to the potentials presented by Zinc oxide nanoparticles.

Materials and Methods

Materials

The *C. aralioides* leaves used in the experiment were given the voucher number DELSU-0301 by a plant taxonomist at Delta State University's Herbarium Unit in Abraka, Delta State, Nigeria. Perkin Elmer Lambda 40 UV-visible Spectrometer, Rigaku D/Max-IIIC and Pelkin Elmer 3000 MX Fourier Transform Infra-red (FTIR) Spectrometer, a powered X-ray diffractometer (PXRD, made by Rigaku Int. Corp. Japan), Scanning Electron Microscope (SEM) (JOEL JSM-7600F), Energy Dispersive X-ray (EDX) (EDX-8100) Spectrometer, and Transmission Electron Microscope (TEM) (JEM-ARM200F-G-TEM) were employed for spectroscopic evaluation.

Staphylococcus aureus, *Escherichia coli*, *Candida albicans*, and *Aspergillus fumigatus* are among the microorganisms that were obtained from the Department of Microbiology at Delta State University, Abraka, Delta State. Gentamycin utilized as positive control medication was obtained from pharmacy store. **Figure 1** displays the flow chart of the procedures followed. Each step's procedures are described in depth.

Evaluation of Phytochemicals and Extraction

Methanol was used in extraction of 200 g of the fresh (paste form) leaf material (at a 1:2 ratio), following Soxhlet extraction method for four h at 55°C. The solvent in the extract combination was evaporated to obtain the crude extract (E3) (10% yield).

The extract was subjected to phytochemical evaluation using the methodology outlined by Jeenu *et al.* (46), Onunkwo (47), and Amina *et al.* (48), to assess if steroids, alkaloids, terpenoids, glycosides, saponin, anthraquinones, proteins, phenolic acids, flavonoids, carbohydrates, tannins, coumarins, and volatile oil, are present.

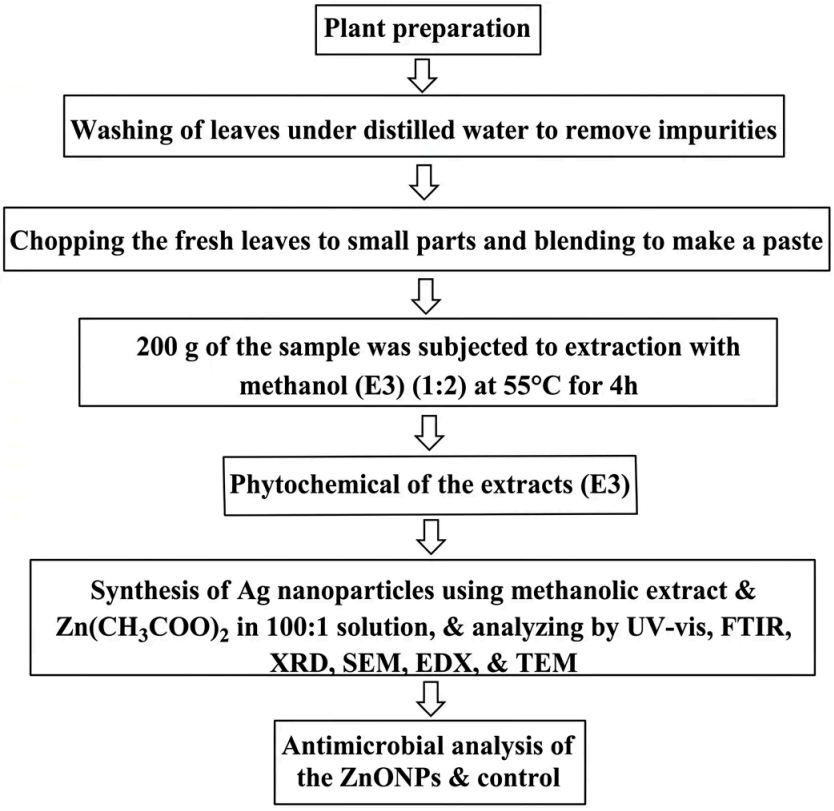

Figure 1. Process flow of the phytochemical extraction and green synthesis of ZnO nanoparticles for antimicrobial applications.

Preparation of the ZnO Nanoparticles

On a magnetic stirrer, 900 mL of 0.02M zinc acetate or $Zn(CH_3COO)_2$ and 9 mL of a 10% (w/v) (100:1) methanolic extract of *C. aralioides* (E3) were mixed together and continuously swirled for 10 min. A 0.5 mL NaOH (1 M) was used to adjust the reaction medium to pH 9 to ensure efficient reduction and stabilization. Using the UV-Vis spectrophotometer, the reduction process of the mixture was monitored until the complete formation and stabilization was reached after 2 h of heating at 70 °C. The resulting ZnONPs solution was then protected from contaminants before purification. After centrifuging the colloidal ZnONPs solution (at 4,000 rpm) and repeatedly washing them using 10 mL of demineralized H_2O, the purified NPs were obtained by oven-drying them for 2 h at 70 to 100 °C (16, 49-50).

Characterizating the ZnO NPs

The NPs' characterization was performed using Ultraviolet-visible spectrophotometer, X-ray Diffraction, FTIR spectrometer, Energy Dispersive X-ray, Scanning Electron Microscope, and Transmission Electron Microscope (TEM) instruments, after necessary preparation were carried out (16, 51).

UV–visible Spectrometry

The spectrometric measurement of biosynthesized ZnO NPs was conducted using a Perkin Elmer Lambda 40 UV-visible spectrophotometer. Using 1 mL of the suspension, the reduction of $Zn(CH_3COO)_2$ was measured at intervals between 200 and 800 nm. Following purification, the sample (purified ZnO NPs) was added 2 mL of deionized water and examined to produce a spectrum of the NPs (16, 52).

Fourier Transform Infrared (FTIR) Spectrometry

The ZnO NPs was dried and purified before being employed. FTIR analysis of the dried ZnO NPs was mixed at a 1:100 (ratio) with an FTIR-grade potassium bromide (KBr) pellet. The spectrometer Pelkin Elmer 3000 MX was used to record the spectrum. There were 32 scans, performed at a resolution (4 cm^{-1}).

Within the range of 4500-300 cm^{-1}, the ZnONPs metal complex's FT-IR spectrum was assessed. The functional group data was obtained by analyzing the infrared spectrum using Win-IR Pro Version 3.0, a spectroscopic program with a 2 cm^{-1} peak sensitivity (16, 49, 52).

X-ray Diffractometry

In order to ascertain the crystallinity of the biologically reduced ZnO NPs (which underwent additional pelletization, powdering, and sieving to 0.074 mm), X-ray diffraction test was performed. The crystallinity of the NPs coated atop glass slides was measured using powered X-ray diffractometer (Rigaku D/Max-IIIC-PXRD) with a CuKa radiation set at 40 kV and 20 mA. The device scanned between 2 and 50 degrees at a rate of 2 degrees per min while operating at room temperature.

Upon passing through the sample, the X-ray produces peaks that are characteristic of the type of diffraction along a set of planes. The peculiarities of the atom arrangement within the sample determine how the peaks are diffracted. The standard data and the diffraction values (d-value and intensity level) were compared. The Debye-Scherrer formula was then used to calculate the ZnO NPs' average particle size (16, 25, 50, 53).

Scanning Electron Microscope (SEM)

SEM is a kind of microscope that creates monographs of samples by using a concentrated electron beam to scan their surfaces. For SEM analysis of the ZnONPs, the JOEL JSM-7600F was used. The pure ZnONPs was placed in the specimen chamber after being conditioned (covered with platinum). The particle was subsequently fixed on the specimen stub (a semiconductor wafer) in order to capture the shape and texture of NPs. The SEM apparatus then placed the specimen in a relatively high-pressure compartment with a short operating distance and an electron optical chamber that is distinctively pumped to maintain a low enough vacuum at the electron gun's edge (16, 25, 50).

Energy Dispersive X-ray (EDX)

The ZnONPs' elemental makeup was assessed by EDX analysis using an EDX-8100 equipment. A thin coating of a copper grid containing ZnO NPs (about 10 mg/mL) was produced, and the NPs' elemental compositions were examined (16).

Transmission Electron Microscope (TEM)

To see the shape of the NPs, Transmission Electron Microscope (TEM) (JEM-ARM200F-G-TEM) was utilized. The device was run with a 200 kV accelerating voltage, a 0.2 nm ultra-high resolution, and a 2,000,000 X magnification. A 3 mm diameter TEM grid was created by applying a sample of the ZnO nanoparticles to a copper grid coated with carbon, allowing it to dry underneath a mercury illumination, and then magnifying the image. The particle size of the ZnONPs was then determined and clear morphological data was provided by using image magnification software to examine the particle size (16, 52).

Antimicrobial Evaluation

The European committee on antimicrobial susceptibility testing-recommended rapid antimicrobial susceptibility testing was followed. Using the agar-well diffusion procedure, the antimicrobial activity of the generated ZnONPs was evaluated at doses of 100, 200, 300, and 400 mg/mL against pathogenic microorganisms (*S. aureus*, *E. coli*, *A. fumigatus*, and *C. albicans*). Cleaning and drying petri dishes were then employed for the research. Various discs immersed in the different concentrations of the materials were arranged outward on their corresponding Mueller-Hinton's agar plates that had been inoculated. Furthermore, the standard antibiotics (Gentamycin) discs were applied at doses of 50, 25, 12.5, and 6.25 mg/mL to prepared *S. aureus*, *E. Coli*, *Aspergillus sp.*, and *C. albicans* microorganisms. Incubation of the discs (at 37°C) was then conducted. The length of the period of incubation varied according to the kind of microbe used against the sample (for example, the incubation period for bacteria was 24 h, but the incubation period for fungi was 5 days). The zone of inhibition (ZOI) was examined and recorded using callipers following incubation. The activity was subjected to duplicate analysis to obtain a preliminary overview of the results and ensure some level of reliability (50, 52, 54-

58).

Results and Discussion

Phytochemical Screening Results

Flavonoids, steroids, alkaloids, phenols, anthraquinones, tannins, terpenoids, proteins, glycosides, volatile oil, and carbohydrates are all present in the methanol leaf extract of *C. aralioides*, but no coumarin was found (**Table 1**). Coumarins are photosensitive and can be degraded by natural light or altered by temperature and storage condition, and this may be the reason why they were undetectable and absent in the extract (59-60).

The plant has been reported to include steroids, alkaloids, tannins, saponins, terpenes, flavonoids, and cardiac glycosides (41, 61). *Cissus hastata* (Semperai), the plant's close specie, has also demonstrated the presence of tannin, phenolic compounds, alkaloids, as well as steroids (62). Alkaloids found in plants have been shown to possess antibacterial qualities (33, 41, 63). Additionally, they can be used to treat skin diseases such seborrheic dermatitis, neurodermatitis, and eczema (33, 41). One of the many anti-inflammatory properties demonstrated by flavonoids, tannins, and steroids was the inhibition of mediators and pathways that cause/induce inflammation and malignancies such as cyclooxygenase, nitric oxide synthase, and lipooxygenase (41, 64).

Table 1. Phytochemicals of methanol leaf extract of C. aralioides (E3).

Phytochemicals	Extract
Alkaloids	+
Saponin	+
Terpenoids	+
Flavonoids	+
Steroids	+
Anthraquinones	+
Glycosides	+
Tannins	+
Phenols	+
Coumarin	-
Proteins	+
Carbohydrates	+
Volatile oil	+
Key: + = Present; - = Absent	

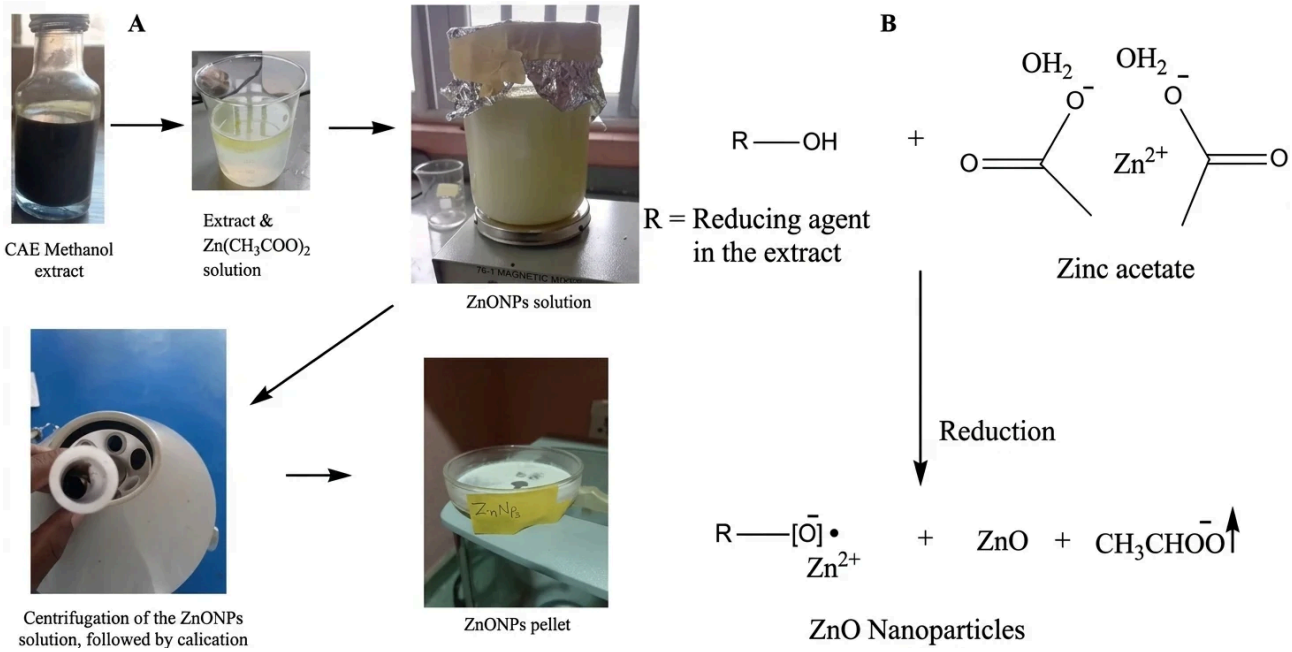

Figure 2. Green synthesis of ZnO nanoparticles: (A) Experimental procedure from CAE methanol extract and (B) Proposed reaction mechanism.

The ZnO NPs'Characteristics

Bioreduction of $Zn(CH_3COO)_2$ to produce ZnO NPs was facilitated by the plant extract's phytochemicals. The formation is confirmed by the UV-visible spectrum. **Figure 2** illustrates the synthetic steps (A) and mechanism (B) of the ZnONPs. The FTIR, XRD, SEM, EDX, and TEM results, are other characteristics results that confirm the nanoparticles.

UV–visible Spectrometry

The first instrument that is frequently used to monitor the development and formation of the nanoparticles is UV-Vis spectrophotometer. This is because the information it offers about the nanoparticles' development is vital. Using a Perkin Elmer Lambda 40 UV-vis spectrometer, the ZnONPs' generation was monitored; the resulting spectrum is displayed in **Figure 3A**.

As seen in the **Figure 3A**, the ZnONPs' UV-vis absorbance spectrum shows a distinct 398 nm (maxmium absorption), slightly above that observed in the work of Akpeji *et al.* (16) but somewhat comparable to what Al-darwesh *et al.* (65) reported. This surface plasmon resonance gave more information on the electronic transitions, shape, size, and aggregation of the NPs. Since the energy of the absorbed photons can be calculated from the peak and may be utilized to assess the optical potential of the NPs, the bandgap (hv/λ) of ZnONPs at 398 nm (absorption maximum) is 1240/398 = 3.12 eV. Energy band gap is important in photonics and semiconductor research (8-9).

Fourier Transform Infrared (FTIR)

The associated functional groups of biomolecules functioning as capping and stabilizing agents on the ZnONPs' surface of were investigated using FTIR analysis. For this study, an Elmer 3000 MX FTIR spectrometer with 4500 – 300 cm^{-1} capacity range was used. **Figure 3B** determines if the functional groups are present on the surface of the nanoparticles, and it displays the chemical characteristics, interactions, and bonding behaviors of the ZnONPs biosynthesised nanoparticles. Al-darwesh *et al.* (65) stated that because of the interactions between its many components, plant extract can promote the creation of the ZnONPs. Aromatic O-H vibrational band of alcohol or phenolic groups is represented by the large peaks at 4028 and 3428 cm^{-1}. Elemike *et al.* (52) had similar report for this vibration. The 2901.57 cm^{-1} sharp peak corresponds to that in primary amine group (N–H) (66). The 2600, and 2358.8 cm^{-1} peaks correspond to that methyl, and methylene groups, respectively (52), while the C≡N (nitrile bond) is attributed to 2144.21 cm^{-1} peak (67). The C=O (carbonyl) bond's stretching vibration may have created a link with the ZnONPs from the flavonoids of the *C. aralioides* extract, as evidenced by the sharp absorption signal detected at 1635.47 cm^{-1}. The 1375.82, 1328.62, and 1439.9 cm^{-1} peaks signal the presence of C–O group. The slight shifting absorption bands at 1157.33 and 1102.36 cm^{-1} may be asserted to nitro (N=O and N–O) group's vibration. The primary alcohol C–H stretch, as also reported by Din *et al.* (66), is shown by 1048.42 cm^{-1} broad peak. The zinc metal-oxygen bond (Zn–O) is identified by the 600.36 and 448 cm^{-1} peaks, and the peaks are comparable to some previous reports (28, 66). Therefore, it can be deduced that this interaction resulted in the formation of the ZnO nanostructure (66, 67). The ZnONPs demonstrated a well-distributed functional group, indicating that its synthesis was complete.

X-ray Diffraction

The ZnONPs' crystal structure and overall oxidation state were investigated using the Powered X-ray diffractometer (Rigaku D/Max-IIIC-PXRD). **Figure 3C** showed the pattern obtained from the XRD of the ZnO nanoparticles prepared with zinc acetate dihydrate and leaf extract from *C. aralioides*. The creation of biologically produced ZnONPs was also confirmed by X-ray diffraction investigation. The diffraction peaks appeared at 2θ scores of 55.00°, 45.05°, 36.02°, 28.05°, 27.00°, and 24.05°, corresponding to (311), (220), (200), (101), (111), and (100) hexagonal/cubic crystal planes.

This is also revealed in a related work by Getie *et al.* (

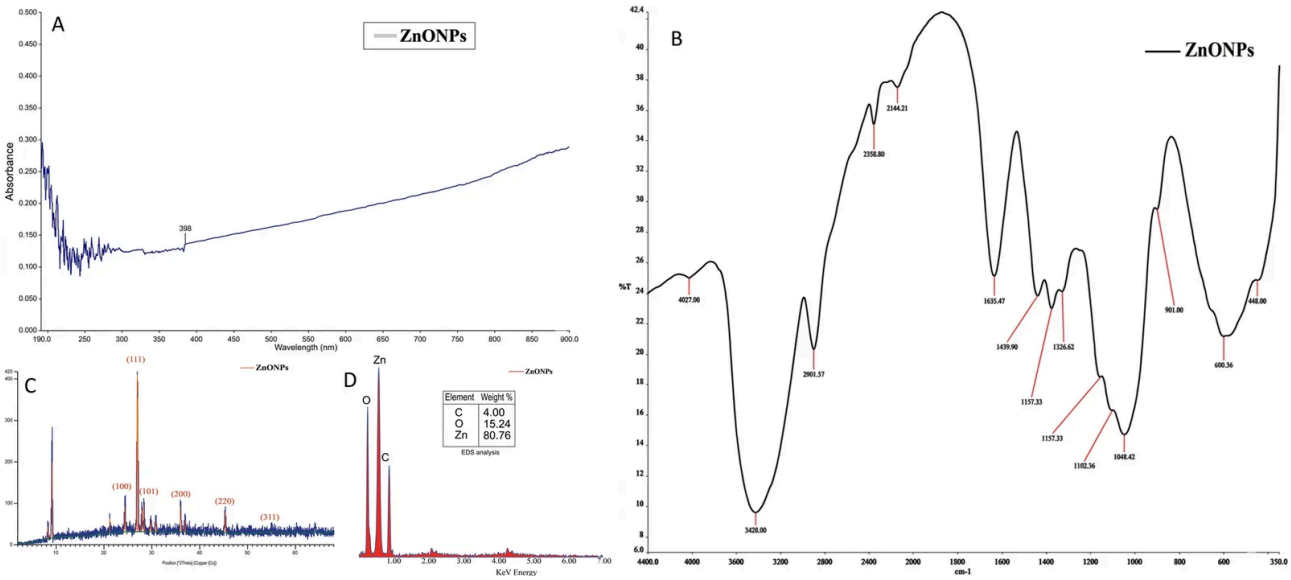

Figure 3. Characterization of ZnO nanoparticles: (A) UV-vis spectrum, (B) FTIR spectrum, (C) PXRD pattern, and (D) EDX spectrum.

68). Although the structure looked more like a cubic blende ZnO structure; however, due to the strain and broadening observed, it can be attributed as a hexagonal wurtzite-like ZnO structure and may be defined by the peak at 36.02°, indexed at (101) (based on the JCPDS card no. 36-1451, and analytical results from its TEM micrograph (**Figure 4B**), and EDX elemental makeup (**Figure 3D**)). Sometimes, XRD patterns of ZnO nanoparticles may show variations in peak intensity, position, and broadening, due to certain specific conditions in their synthesis and so on (69-70). The crystallization of bioorganic components on the surface of NPs was linked to the non-indexed spikes at 37.00°, 28.09°, 21.05°, and 9.05° (71-73).

Debye-Scherrer formula, $D = K\lambda/\beta\cos\theta$, was used to determine the crystalline size. Here, λ stands for the X-ray wavelength, K for the Scherrer constant, θ for the Bragg angle, and β for the diffraction peak's full width at half maximum (FWHM) (in radians). This study's computed crystalline size of 28.31 nm for ZnONPs was slightly larger than that discovered by Waseem and Divya (7), but it was similar to that published by Demissie *et al.* (28).

Energy Dispersive X-ray (EDX)

The elemental structure of the produced ZnO nanoparticles was investigated utilizing the EDX-8100 equipment. The EDX analysis results of the bio-synthesized ZnONPs displayed the various elemental makeup and their percentages. Zinc (80.76%), and oxygen (15.24%) were the predominant elements, followed by elemental carbon (4.00%), as displayed in **Figure 3D**.

The presence of these fundamental elements suggests the involvement of organic constituents, likely obtained from the extract's biomolecules, in the formation (67). According to Akpeji *et al.* (74), the extract is responsible for the carbon present in the nanoparticles.

Scanning Electron Microscope (SEM)

SEM was utilized to view the microscopic image of the bio-generated NPs. The shape of the ZnONPs was found to have an uneven and rough surface (**Figure 4A**), from the SEM analysis using SEM (JOEL JSM-7600F) equipment. According to Akpeji *et al.* (74), this is the outcome of interactions between the surrounding medium and the surface of the nanoparticles. These exchanges are thought to result from the extract's functional groups serving as stabilizers during the biosynthetic process (16, 67).

Transmission Electron Microscope (TEM)

The shape of the NPs and, more crucially, their particle sizes are clearly depicted by TEM analysis with TEM model JEOL2100 equipment. The Origin Lab software (version 9.0), and imageJ, were employed to calculate the bio-synthesized ZnONPs' average particle size. **Figure 4B** showed the TEM micrograph of the ZnO NPs. It is somewhat agglomerated, featuring a wurtzite-like hexagonal structure with some hazy and dark areas. This depiction is in agreement with that obtained by Demissie *et al.* (28). The metal and organic component regions may be responsible for the observed dark and bleak areas (75-76). The scale of 50 nm was used to visualize the nanoparticles, and a little overlapping was observed in some areas of the particle's image. The size of the nanoparticles showed that they had a very wide surface area, which explains their many applications in adsorption experiments, including studies involving harmful microorganisms at the surface of the nanoparticles, in addition to their roles in chemical reactions (74, 76). From the imageJ (resolution analyzer) and Origin Lab application softwares, the the calculated ZnONPs' average particle size is 15.90 nm, as seen in the histogram (**Figure 4C**). This average particle size coincides with one of the values recorded by Akpeji *et al.* (75), however, it is slightly smaller than that found by Demissie *et al.* (28). Generally, the crystallite size (from XRD) is smaller than or equal to particle size (from TEM/SEM); however, the average crystallite size of ZnO NPs here appears bigger than the particle size. This discrepancy may likely be due to instrumental broadening errors, as strain within the lattice can broaden peaks (in XRD), or because the TEM technique may have only imaged smaller fragments or a subset of the true particles, or the surface coating on biologically synthesized nanoparticles might be thin or not visible in TEM (77-78).

Antimicrobial Activity Result

Table 2, and **Figure 5A** showed that the ZnO NPs from *C. aralioides* leaf extract was highly active against all the microbes, with the highest and lowest activity obtained at 24, and 8 mm, respectively. The nanoparticles showed more sensitivity against *S. aureus*, with the 100-300 mg/mL displaying 16 mm inhibitory, and 400 mg/mL demonstrating the highest sensitivity of 24 mm. There were 22, and 20 mm inhibitory effects observed against *C. albicans*, and *E. coli*, respectively at 400 mg/mL, and the effects on each of the organisms at 200 to 300 mg/mL

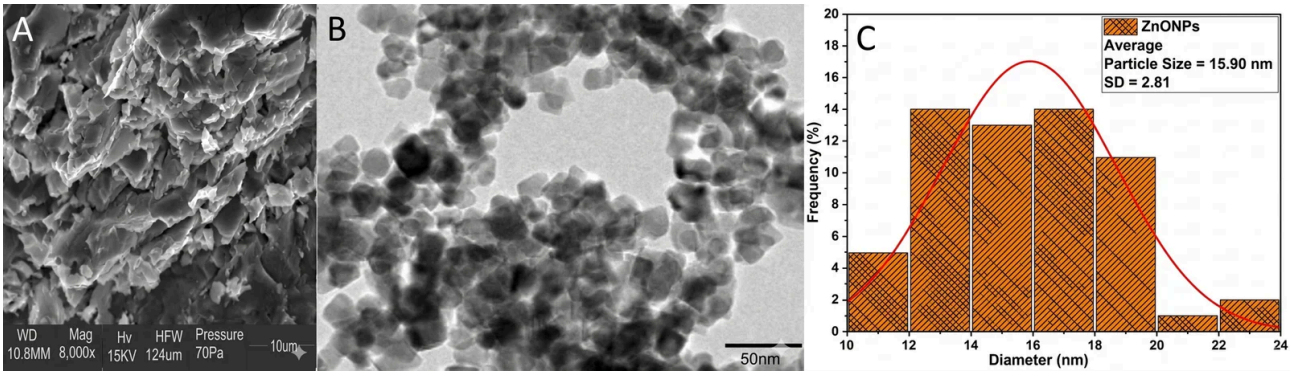

Figure 4. Morphological analysis of ZnO nanoparticles: (A) SEM micrograph showing surface morphology, (B) TEM image revealing particle shape and internal structure, and (C) Particle size distribution histogram derived from TEM analysis.

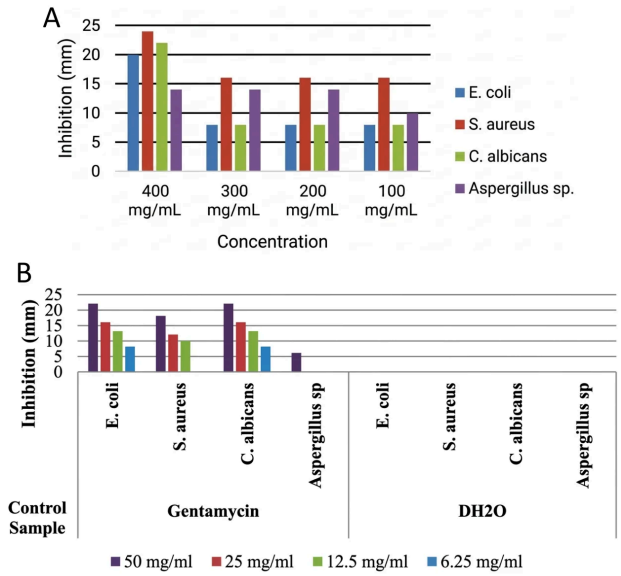

Figure 5. *In vitro* antimicrobial activity evaluation: (A) Inhibition zones of ZnO nanoparticles against target pathogens and (B) Comparative sensitivity of Gentamycin as a positive control.

stood at 8 mm. The nanoparticles showed a random inhibitory activity against *Aspergillus sp.*, with a 10 mm resistance at 100 mg/mL, and a 14 mm inhibitory effect at 200-400 mg/mL concentrations. The reason why 400 mg/mL demonstrated the highest sensitivity due to increased concentration which results to greater inhibition (28).

The results for the ZnO NPs'antimicrobial activity, when compared to the positive control, Gentamycin (**Table 3** and **Figure 5B**) were somewhat comparable at their highest concentration, indicating the sample's efficacy as the concentrations are increased. Waseem and Divya (7) reported the results that differed slightly from this research. Getie *et al.* (68), and Al-darwesh *et al.* (65) stated that zinc oxide nanostructure showed great antibacterial activity against several microbes. The enhanced surface area, which contributes to improved bioavailability, allowed the nanoparticles to penetrate the microorganisms'cell walls and more successfully interact with their enzymes, causing cellular harm by preventing their growth and biological functions (67, 79-81). The antimicrobial activity may be attributed to a possible release of Zn^{2+} from the ZnO NPs into the cell walls of the microbes to inhibit their several cellular activities like active transport, metabolism, and enzyme activity, leading to cell death due to the potential toxicity of Zn^{2+}. This release of Zn^{2+} from ZnO NPs is one of the main propositions in antibacterial mechanisms (28). Also, Agarwal *et al.* (82) stated that antibacterial activity of ZnO NPs can be caused by the formation of reactive oxygen

Table 2. Antimicrobial activity of ZnO nanoparticles at various concentrations against different pathogenic microorganisms.

Sample	Organism	Concentration (mg/mL)			
		400	300	200	100
ZnONPs	*E. coli*	20.0 ± 0.01^{a}	8.0 ± 0.04^{b}	8.0 ± 0.02^{b}	8.0 ± 0.01^{b}
	S. aureus	24.0 ± 0.01^{a}	16.0 ± 0.04^{b}	16.0 ± 0.02^{b}	16.0 ± 0.01^{b}
	C. albicans	22.0 ± 0.01^{a}	8.0 ± 0.04^{b}	8.0 ± 0.02^{b}	8.0 ± 0.01^{b}
	Aspergillus sp	14.0 ± 0.04^{a}	14.0 ± 0.02^{a}	14.0 ± 0.01^{a}	10.0 ± 0.01^{b}

Note: The value is Mean ± SD; For a Tukey's HSD test, the same letters in the same row are not significantly different ($p < 0.05$) for each of the parameters (data) evaluated

Table 3. Sensitivity of pathogenic microorganisms to positive (Gentamycin) and negative (DH_2O) controls at various concentrations.

Control	Organism	Unit	Concentration (mg/mL)			
			50	25	12.5	6.25
Gentamycin	*E. coli*	mm	22.0 ± 0.01^{a}	16.0 ± 0.04^{b}	13.0 ± 0.04^{c}	8.0 ± 0.04^{d}
	S. aureus		18.0 ± 0.01^{a}	12.0 ± 0.01^{b}	10.0 ± 0.01^{c}	0.0 ± 0.00^{d}
	C. albicans		22.0 ± 0.01^{a}	16.0 ± 0.01^{b}	13.0 ± 0.01^{c}	8.0 ± 0.04^{d}
	Aspergillus sp		6.0 ± 0.01^{a}	0.0 ± 0.00^{b}	0.0 ± 0.00^{b}	0.0 ± 0.00^{b}
DH2O	*E. coli*	mm	0.0 ± 0.00^{a}	0.0 ± 0.00^{a}	0.0 ± 0.00^{a}	0.0 ± 0.00^{a}
	S. aureus		0.0 ± 0.00^{a}	0.0 ± 0.00^{a}	0.0 ± 0.00^{a}	0.0 ± 0.00^{a}
	C. albicans		0.0 ± 0.00^{a}	0.0 ± 0.00^{a}	0.0 ± 0.00^{a}	0.0 ± 0.00^{a}
	Aspergillus sp		0.0 ± 0.00^{a}	0.0 ± 0.00^{a}	0.0 ± 0.00^{a}	0.0 ± 0.00^{a}

Note: The value is Mean±SD; For a Tukey's HSD test, the same letters in the same row are not significantly different ($p < 0.05$) for each of the parameters (data) evaluated.

species (ROS) which leads to oxidative stress and subsequent cell damage or death. According to Demissie *et al*. (28), the possible mechanism for the antimicrobial activity of ZnO NPs is through the attachment of NPs to the bacteria cell membrane via electrostatic forces. Then, the interaction distorts the membrane plasma structure and damages the bacterial cell integrity, resulting in the leakage of intracellular contents and ends with cell death.

However, cytotoxicity studies focusing on mechanisms like oxidative stress, mitochondrial damage, and membrane disruption are needed to evaluate how the NPs' size, shape, surface charge, and coating affect cell viability. Some of the studies including ROS generation measurements to determine safe concentrations, MTT (3-(4,5-dimethylthiazol-2-yl)-2,5-diphenyltetrazolium bromide) reduction assay to cell viability based on metabolic activity, LDH release assay to evaluates cell damage by measuring lactate dehydrogenase release, and flow cytometry to examines cell cycle, apoptosis (Annexin V/Propidium iodide), and NPs' uptake, are essential for deeper understanding (83).

Conclusion

Zinc oxide NPs was successfully created in this study using methanol leaf extract of *C. aralioides*. The plant extract's phytochemicals functioned as capping and stabilizing agents and successfully generated the NPs. TEM, EDX, SEM, PXRD, FTIR, and UV-vis confirmed the NPs' characteristic results. The green-synthesized ZnONPs showed a maximum absorption of 398 nm and calculated bandgap energy of 3.12 eV. Its average particle size, as determined by the hexagonal wurtzite-like form was 15.90 ± 2.81 nm, and its crystalline size was 28.31 nm on average. For the SEM data, a rough and uneven surface morphology was confirmed, and the EDX result showed that the predominant element was Zn (80.76%). The plant's abundance of vital phytochemicals with disease-fighting properties is evidenced by the existence of many vibrational groups found through the FTIR investigation. The NPs recorded promising results against *S. aureus*, *E. coli*, *Aspergillus sp*., and *C. albicans* from the antimicrobial activity assay. The ZnO nanoparticles showed strong action against the microorganism, although *C. aureus* was the one that was most affected (at 22.0 ± 0.01 mm). By estimate, 200–100 mg/mL was the minimum inhibitory concentration. At higher concentrations, the positive control outperformed the sample but still displayed similar inhibitions.

Further, future works can look into conducting stability measurements, zeta potentials, and size distribution analysis on the ZnO NPs. Also, mechanistic ROS assays or membrane damage studies, and antimicrobial analysis that involves comparison of the ZnO NPs with the plant extract should be undertaken. Again, FTIR analysis of the plant extract, and other studies of the nanoparticles in biomedicines, medicine, photocatalysis, semiconductors fabrications, electronics, bioremediation, automobiles, agriculture, computer technology, and energy production and storage are also reframed for future investigations.

Overall, the findings have shown that infectious microbes can be controlled by ZnO nanoparticles. From the present study, the findings suggest that the produced ZnONPs can be employed as an antimicrobial agent to manage infections.

Declaration

Author Information

Innocent Chukwujekwu Onunkwo
*Corresponding author
Department of Industrial Chemistry, Nigeria Maritime University, Okerenkoko, Delta State, Nigeria..
Contribution: Conceptualization, Funding acquisition, Investigation, Methodology, Writing - Original Draft.

Mary Olire Edema
Department of Chemistry, Federal University of Petroleum Resources, Effurun, Delta State, Nigeria..
Contribution: Supervision, Validation, Writing - Review & Editing.

Christiana E. Ogwuche
Department of Chemistry, Federal University of Petroleum Resources, Effurun, Delta State, Nigeria..
Contribution: Project administration, Resources, Validation, Writing - Original Draft.

Bamidele H. Akpeji
Department of Science Lab Tech (SLT), Federal University of Petroleum Resources, Effurun, Delta State, Nigeria. .
Contribution: Investigation, Writing - Original Draft.

Acknowledgment

The authors wish to thank TETFUND' Executive Secretary for fund the agency provided for the research. The management of Nigeria Maritime University in Okerenkoko and the Federal University of Petroleum Resources in Effurun, Delta State, Nigeria, are also acknowledged for providing the platforms and opportunity to conduct this research.

Conflict of Interest

The authors declare no conflicting interest.

Data Availability

The data generated during and/or analyzed during the current study are available from the corresponding author on reasonable request.

Ethics Statement

Ethical approval was not required for this study.

Funding Information

This work was supported by the Tertiary Education Trust Fund, NG under Grant Number TETFUND/AST&D/2023/BatchD.

References

1. Medina Cruz D, Mostafavi E, Vernet-Crua A, Barabadi H, Shah V, Cholula-Díaz JL, *et al*. Green nanotechnology-based zinc oxide (ZnO) nanomaterials for biomedical applications: a review. J. Phys. Mater. 2020;3(3):034005. doi: https://doi.org/10.1088/2515-7639/ab8186

2. Kalpana VN, Devi Rajeswari V. A Review on Green

Synthesis, Biomedical Applications, and Toxicity Studies of ZnO NPs. Bioinorganic Chemistry and Applications. 2018;2018(1):1-12. doi: https://doi.org/10.1155/2018/3569758

3. Abbasi BH, Shah M, Hashmi SS, Nazir M, Naz S, Ahmad W, *et al*. Green Bio-Assisted Synthesis, Characterization and Biological Evaluation of Biocompatible ZnO NPs Synthesized from Different Tissues of Milk Thistle (Silybum marianum). Nanomaterials. 2019;9(8):1171. doi: https://doi.org/10.3390/nano9081171

4. Gao Y, Xu D, Ren D, Zeng K, Wu X. Green synthesis of zinc oxide nanoparticles using Citrus sinensis peel extract and application to strawberry preservation: A comparison study. Lwt. 2020;126(10):109297. doi: https://doi.org/10.1016/j.lwt.2020.109297

5. Muthuvinothini A, Stella S. Green synthesis of metal oxide nanoparticles and their catalytic activity for the reduction of aldehydes. Process Biochemistry. 2019;77(2):48-56. doi: https://doi.org/10.1016/j.procbio.2018.12.001

6. Onunkwo IC, Edema MO, E. Ogwuche C, A. Enemose E. Biosynthesis of silver nanoparticles using Cissus aralioides Methanol leaf extract and antimicrobial application. Int. J. Sci. Res. Updates. 2026;11(1):020-033. doi: https://doi.org/10.53430/ijsru.2026.11.1.0013

7. Ahmad W, Kalra D. Green synthesis, characterization and anti microbial activities of ZnO nanoparticles using Euphorbia hirta leaf extract. Journal of King Saud University - Science. 2020;32(4):2358-2364. doi: https://doi.org/10.1016/j.jksus.2020.03.014

8. Lee GH. Morphology and luminescence properties of ZnO micro/nanostructures synthesized via thermal evaporation of Zn–Mg mixtures. Ceramics International. 2015;41(7):8475-8480. doi: https://doi.org/10.1016/j.ceramint.2015.03.053

9. Kim E, Kim M, Im N, Park S. Photolysis of the organic UV filter, avobenzone, combined with octyl methoxycinnamate by nano-TiO2 composites. Journal of Photochemistry and Photobiology B: Biology. 2015;149(8)196-203. doi: https://doi.org/10.1016/j.jphotobiol.2015.05.011

10. Chebil W, Boukadhaba M, Fouzri A. Epitaxial growth of ZnO on quartz substrate by sol-gel spin-coating method. Superlattices and Microstructures. 2016;95(7):48-55. doi: https://doi.org/10.1016/j.spmi.2016.04.033

11. Inguva S, Gray C, McGlynn E, Mosnier JP. Origin of the 3.331 eV emission in ZnO nanorods: Comparison of vapour phase transport and pulsed laser deposition grown nanorods. Journal of Luminescence. 2016;175(10):117-121. doi: https://doi.org/10.1016/j.jlumin.2016.02.027

12. Shewale P, Yu Y. The effects of pulse repetition rate on the structural, surface morphological and UV photodetection properties of pulsed laser deposited Mg-doped ZnO nanorods. Ceramics International. 2016;42(6):7125-7134. doi: https://doi.org/10.1016/j.ceramint.2016.01.101

13. Sreedhar A, Kwon JH, Yi J, Kim JS, Gwag JS. Enhanced photoluminescence properties of Cu-doped ZnO thin films deposited by simultaneous RF and DC magnetron sputtering. Materials Science in Semiconductor Processing. 2016;49(11):8-14. doi: https://doi.org/10.1016/j.mssp.2016.03.023

14. Ali SG, Ansari MA, Khan HM, Jalal M, Mahdi AA, Cameotra SS. Antibacterial and Antibiofilm Potential of Green Synthesized Silver Nanoparticles against Imipenem Resistant Clinical Isolates of P. aeruginosa. BioNanoSci. 2018;8(2):544-553. doi: https://doi.org/10.1007/s12668-018-0505-8

15. Ansari MA, Alzohairy MA. One-Pot Facile Green Synthesis of Silver Nanoparticles Using Seed Extract of *Phoenix dactylifera* and Their Bactericidal Potential against MRSA. Evidence-Based Complementary and Alternative Medicine. 2018;2018(1):1860280. doi: https://doi.org/10.1155/2018/1860280

16. Akpeji BH, Emegha MC, Onyenue EE, Meshack OQ, Elemike EE. Synthesis and Characterization of Nanoparticles of Zno, Carbon Dot and Zno-Carbon Dot Nanocomposite from Groundnut Shell Wastes. jasem. 2024;28(6):1771-1780. doi: https://doi.org/10.4314/jasem.v28i6.16

17. Selim S, Saddiq AA, Ashy RA, Baghdadi AM, Alzahrani AJ, Mostafa EM, *et al*. Bimetallic selenium/zinc oxide nanoparticles: biological activity and plant biostimulant properties. AMB Expr. 2025;15(1):1-17. doi: https://doi.org/10.1186/s13568-024-01808-y

18. Nilavukkarasi M, Vijayakumar S, Prathipkumar S. Capparis zeylanica mediated bio-synthesized ZnO nanoparticles as antimicrobial, photocatalytic and anti-cancer applications. Materials Science for Energy Technologies. 2020;3(1):335-343. doi: https://doi.org/10.1016/j.mset.2019.12.004

19. Tabrizi Hafez Moghaddas SM, Elahi B, Javanbakht V. Biosynthesis of pure zinc oxide nanoparticles using Quince seed mucilage for photocatalytic dye degradation. Journal of Alloys and Compounds. 2020;821(10):153519. doi: https://doi.org/10.1016/j.jallcom.2019.153519

20. Mohd Yusof H, Mohamad R, Zaidan UH, Abdul Rahman NA. Microbial synthesis of zinc oxide nanoparticles and their potential application as an antimicrobial agent and a feed supplement in animal industry: a review. J Animal Sci Biotechnol. 2019;10(1):1-22. doi: https://doi.org/10.1186/s40104-019-0368-z

21. Vijayakumar S, Arulmozhi P, Kumar N, Sakthivel B, Prathip Kumar S, Praseetha P. Acalypha fruticosa L. leaf extract mediated synthesis of ZnO nanoparticles: Characterization and antimicrobial activities. Materials Today: Proceedings. 2020;23(13):73-80. doi: https://doi.org/10.1016/j.matpr.2019.06.660

22. Chakraborty SS, Panja A, Dutta S, Patra P. Advancements in nanoparticles for skin care: a comprehensive review of properties, applications, and future perspectives. Discov Mater. 2024;4(1):1-23. doi: https://doi.org/10.1007/s43939-024-00088-4

23. Omeh RC, Ali IJ, Adonu CC, Ogbonna JI, Ugorji LO, Mbah CC, *et al*. Green Synthesis of Zinc Oxide Nanoparticles Characterization and Use for Formulation of Sunscreen Topical Creams. Trop J Nat Prod Res. 2025;9(6):2384-2394. doi: https://doi.org/10.26538/tjnpr/v9i6.5

24. Onunkwo I, Edema M, Ogwuche C. Cissus aralioides Leaf: Cosmetological Application of the Methanol extract, Its Silver and Zinc Oxide Nanoparticles and Characterization. Chem Pap. 2025;80(3):3213-3234. doi: https://doi.org/10.21203/rs.3.rs-7942449/v1

25. Elemike EE, Onwudiwe DC, Mbonu JI. Facile synthesis of cellulose–ZnO-hybrid nanocomposite using Hibiscus rosa-sinensis leaf extract and their antibacterial activities. Appl Nanosci. 2021;11(4):1349-1358. doi: https://doi.org/10.1007/s13204-021-01774-y

26. Ansari MA, Murali M, Prasad D, Alzohairy MA, Almatroudi A, Alomary MN, *et al*. Cinnamomum verum Bark Extract Mediated Green Synthesis of ZnO Nanoparticles and Their Antibacterial Potentiality. Biomolecules. 2020;10(2):336. doi: https://doi.org/10.3390/biom10020336

27. Chaudhary A, Kumar N, Kumar R, Salar RK. Antimicrobial activity of zinc oxide nanoparticles synthesized from Aloe vera peel extract. SN Appl. Sci. 2018;1(1):136. doi: https://doi.org/10.1007/s42452-018-0144-2

28. Demissie MG, Sabir FK, Edossa GD, Gonfa BA. Synthesis of Zinc Oxide Nanoparticles Using Leaf Extract of Lippia adoensis (Koseret) and Evaluation of Its Antibacterial Activity. Journal of Chemistry. 2020;2020(1):1-9. doi: https://doi.org/10.1155/2020/7459042

29. Elumalai K, Velmurugan S, Ravi S, Kathiravan V, Ashokkumar S. RETRACTED: Green synthesis of zinc oxide nanoparticles using Moringa oleifera leaf extract and evaluation of its antimicrobial activity. Spectrochimica Acta Part A: Molecular and Biomolecular Spectroscopy. 2015;143(12):158-164. doi: https://doi.org/10.1016/j.saa.2015.02.011

30. Ogunyemi SO, Abdallah Y, Zhang M, Fouad H, Hong X, Ibrahim E, *et al*. Green synthesis of zinc oxide nanoparticles using different plant extracts and their antibacterial activity against *Xanthomonas oryzae* pv. oryzae. Artificial Cells, Nanomedicine, and Biotechnology. 2019;47(1):341-352. doi: https://doi.org/10.1080/21691401.2018.1557671

31. Bongers F, Parren MPE, Traoré D, editors. Forest climbing plants of West Africa: diversity, ecology and management. Wallingford: Cabi; 2005. doi: https://doi.org/10.1079/9780851999142.0000

32. Catarino L, Havik PJ, Romeiras MM. Medicinal plants of Guinea-Bissau: Therapeutic applications, ethnic diversity and knowledge transfer. Journal of Ethnopharmacology. 2016;183(7):71-94. doi: https://doi.org/10.1016/j.jep.2016.02.032

33. Oduje AA, Awode A, Edah A, Sagay I. Characterization and phytochemical screening of n-hexane oil extract from Cissus aralioides seeds. Int J of Sci & Eng Res. 2015;6(1):112-116. https://www.ijser.org/researchpaper/Characterization-and-Phytochemical-Screening-of-n-Hexane.pdf

34. Assob JC, Kamga HL, Nsagha DS, Njunda AL, Nde PF, Asongalem EA, *et al*. Antimicrobial and toxicological activities of five medicinal plant species from Cameroon Traditional Medicine. BMC Complement Altern Med. 2011;11(1):70. doi: https://doi.org/10.1186/1472-6882-11-70

35. Chen B, McClements DJ, Decker EA. Design of Foods with Bioactive Lipids for Improved Health. Annu. Rev. Food Sci. Technol. 2013;4(1):35-56. doi: https://doi.org/10.1146/annurev-food-032112-135808

36. Chukwuebuka N, Kelechi A, Nwanneamaka E, Stephen U. Toxicity Studies and Phytochemical Screening of Aqueous Extract of Cissus aralioides Plant. Jamps. 2018;17(1):1-7. doi: https://doi.org/10.9734/jamps/2018/41425

37. Orakwue FC, Maduanusi AB. Phytochemical and antimicrobial screening of methanol extract of Cissus aralioides. Int J of Sci Innovat. 2014;6(1):65-68. https://www.researchgate.net/profile/Foster-Orakwue/publication/333670960_Phytochemical_and_antimicrobial_screening_of_the_methanol_extract_of_Cissus_aralioides_stem/links/5cfd764092851c874c5b4e6a/Phytochemical-and-antimicrobial-screening-of-the-methanol-extract-of-Cissus-aralioides-stem.pdf

38. Al-Mamary M, Al-Habori M, Al-Zubairi AS. The *in vitro* antioxidant activity of different types of palm dates (Phoenix dactylifera) syrups. Arabian Journal of Chemistry. 2014;7(6):964-971. doi: https://doi.org/10.1016/j.arabjc.2010.11.014

39. Olaoye S. B, Ibrahim A. O, Zhiqiang L. Chemical compositions and radical scavenging potentials of essential oils from*Tragia benthamii*(BAKER) and*Cissus aralioides*(WELW). Journal of Biologically Active Products from Nature. 2016;6(1):59-64. doi: https://doi.org/10.1080/22311866.2016.1175319

40. Ren-You GR, Xiang-Rong X, Feng-Lin S, Lei S, Hua-Bin L. Antioxidant activity and total phenolic content of medicinal plants associated with prevention and treatment of cardiovascular and cerebrovascular diseases. J Med Plants Res. 2010;4:2438-2444. doi: https://doi.org/10.5897/JMPR10.581

41. Ezeja MI, Omeh YN, Onoja SO, Ukaonu IH. Anti-inflammatory and antioxidant activities of the methanolic leaf extract of Cissus aralioides. Am J of Pharmacol Sci.

2015;3(1):1-6. https://doi.org/10.12691/ajps-3-1-1. https://share.google/VOOYB8GvpI6Bc8bgk

42. Ezeja MI, Onoja SO, Ukwueze CO, Madubuike GI. Evaluation of the analgesic activity of Cissus aralioides leaves in rat. J of Chemical & Pharma Res. 2015;7(3):2525-2528. https://share.google/2VVI0vVZSzvg8RKDf

43. Anosike CA, Obidoa O, Ezeanyika LUS. The anti—inflammatory activity of garden egg (Solanum aethiopicum) on egg albumin—induced oedema and granuloma tissue formation in rats. Asian Pacific Journal of Tropical Medicine. 2012;5(1):62-66. doi: https://doi.org/10.1016/s1995-7645(11)60247-2

44. Anosike CA, Ako AC, Nwodo OFC. Anti-inflammatory and membrane stabilization activities of methanol extract of Cissus aralioides leaves. Res J of Pharm Biol & Chem Sci. 2018;18:28. https://www.researchgate.net/publication/339830156_Anti-Inflammatory_And_Membrane_Stabilization_Activities_Of_Methanol_Extract_of_Cissus_aralioides_leaves

45. Nago RDT, Simo Mpetga JD, Tamokou J, Tanemossu Fobofou SA, Mbahbou Bitchagno GT, Wessjohann LA, *et al.* A New Ceramide from *Cissus Aralioides* Baker (Vitaceae) and its Antimicrobial Activity. Chemistry & Biodiversity. 2022;20(1):e202200678. doi: https://doi.org/10.1002/cbdv.202200678

46. Joseph J, Bindhu A, Aleykutty N. *In vitro* and *in vivo* antiinflammatory activity of Clerodendrum paniculatum linn. leaves. Indian J Pharm Sci. 2013;75(3):376. doi: https://doi.org/10.4103/0250-474x.117428

47. Onunkwo IC. A handbook of organic chemistry practical: Tests, procedures and results. XS publishers, Warri, Delta State, Nigeria, ISBN: 9789785873221, 2021. 1-70. https://share.google/ZprxI31NlRCRg5Z1O

48. Amina R, Aliero B, Gumi M. Phytochemical screening and oil yield of a potential herb, camel grass (Cymbopogon schoenanthus Spreng.). Cent Euro J of Experi Biol. 2013;2(3):15b-19. https://share.google/F3LnKOsLWZsAXmTgx

49. Singh R, Navneet. Green synthesis of silver nanoparticles using methanol extract of Ipomoea carnea Jacq. to combat multidrug resistance bacterial pathogens. Current Research in Green and Sustainable Chemistry. 2021;4(7):100152. doi: https://doi.org/10.1016/j.crgsc.2021.100152

50. Ogwuche CE, Moses HO. Characterization, antimicrobial and toxicity studies of silver nanoparticles using Opuntia ficus indica leaves extracts from Effurun, Delta State. Tanzania J of Sci. 2021;47(1):34-46. https://dx.doi.org/10.4314/tjs.v47i1.4

51. Narayanan M, hussain FAJ, Srinivasan B, Sambantham MT, Al-Keridis LA, AL-mekhlafi FA. Green synthesizes and characterization of copper-oxide nanoparticles by Thespesia populnea against skin-infection causing microbes. Journal of King Saud University - Science. 2022;34(3):101885. doi: https://doi.org/10.1016/j.jksus.2022.101885

52. Emeka EE, Ojiefoh OC, Aleruchi C, Hassan LA, Christiana OM, Rebecca M, *et al.* Evaluation of antibacterial activities of silver nanoparticles green-synthesized using pineapple leaf (Ananas comosus). Micron. 2014;57(2):1-5. doi: https://doi.org/10.1016/j.micron.2013.09.003

53. Banala RR, Nagati VB, Karnati PR. Green synthesis and characterization of Carica papaya leaf extract coated silver nanoparticles through X-ray diffraction, electron microscopy and evaluation of bactericidal properties. Saudi Journal of Biological Sciences. 2015;22(5):637-644. doi: https://doi.org/10.1016/j.sjbs.2015.01.007

54. Zainab, Khan MS, Ahmad M, Khan MA, SobiIn. *In vitro* antimicrobial activity of Rumex Dentatus L. (Polygonaceae) plant extracts. Phytopharmacol Res J. 2022;1(3):32-42. https://www.researchgate.net/publication/366642920_In_vitro_antimicrobial_activity_of_Rumex_Dentatus_L_Polygonaceae_plant_extracts

55. Park JM, Kwon M, Hong KH, Lee H, Yong D. European Committee on Antimicrobial Susceptibility Testing-Recommended Rapid Antimicrobial Susceptibility Testing of *Escherichia coli*, *Klebsiella pneumoniae*, and *Staphylococcus aureus* From Positive Blood Culture Bottles. Ann Lab Med. 2023;43(5):443-450. doi: https://doi.org/10.3343/alm.2023.43.5.443

56. Naiel B, Fawzy M, Halmy MWA, Mahmoud AED. Green synthesis of zinc oxide nanoparticles using Sea Lavender (Limonium pruinosum L. Chaz.) extract: characterization, evaluation of anti-skin cancer, antimicrobial and antioxidant potentials. Sci Rep. 2022;12(1):20370. doi: https://doi.org/10.1038/s41598-022-24805-2

57. Ashaduzzaman M, Al Muhit MA, Dey SC, Rahaman MM, Mahmudul Hasan HN, Mustary N, *et al.* Microwave assisted starch stabilized green synthesis of zinc oxide nanoparticles for antibacterial and photocatalytic applications. Sci Rep. 2025;15(1):28288. doi: https://doi.org/10.1038/s41598-025-14193-8

58. Umar M, Ahmad M, Sadeeq M, Ali H, Khan A, Chaudry AA, *et al.* Green synthesis and characterizations of zinc oxide nanoparticles using acorn fruit extract for antimicrobial, larvicidal and *in silico* activities. Sci Rep. 2026;16(1):7072. doi: https://doi.org/10.1038/s41598-026-36137-6

59. Sharifi-Rad J, Cruz-Martins N, López-Jornet P, Lopez EPF, Harun N, Yeskaliyeva B, *et al.* Natural Coumarins: Exploring the Pharmacological Complexity and Underlying Molecular Mechanisms. Oxidative Medicine and Cellular Longevity. 2021;2021(1):6492346. doi: https://doi.org/10.1155/2021/6492346

60. Wang Y, Guan T, Yue X, Yang J, Zhao X, Chang A, *et al.* The biosynthetic pathway of coumarin and its genetic regulation in response to biotic and abiotic stresses. Front. Plant Sci. 2025;16(6):1599591. doi: https://doi.org/10.3389/fpls.2025.1599591

61. Borokini TI. Phytochemical and ethnobotanical study of some selected medicinal plants from Nigeria. J. Med. Plants Res. 2012;6(7):1106-1118. doi: https://doi.org/10.5897/jmpr09.430

62. Muhamad M, Ai Sze W, Zulkifli N, Ab-Rahim S. Qualitative Analysis on the Phytochemical Compounds and Total Phenolic Content of Cissus hastata (Semperai) Leaf Extract. IJPB. 2022;14(1):53-62. doi: https://doi.org/10.3390/ijpb14010005

63. Zhao X, Hu X, Xie Q, Qi S, Xiang Z, Sun X, *et al*. Ameliorative effect of scopolamine-induced cognitive dysfunction by Fufangmuniziqi formula: The roles of alkaloids, saponins, and flavonoids. J Ethnopharmacol. 2024;318(1):116792. doi: https://doi.org/10.1016/j.jep.2023.116792

64. Elemike EE, Onunkwo IC, Ughumiakpor O, Alawuru F, Mukoro A, Ishom P, *et al*. Bio-nanomaterials: Promising anticancer properties and treatment strategies. Nano TransMed. 2025;4(1):100076. doi: https://doi.org/10.1016/j.ntm.2025.100076

65. Al-darwesh MY, Ibrahim SS, Mohammed MA. A review on plant extract mediated green synthesis of zinc oxide nanoparticles and their biomedical applications. Results in Chemistry. 2024;7(1):101368. doi: https://doi.org/10.1016/j.rechem.2024.101368

66. Din MI, Jabbar S, Najeeb J, Khalid R, Ghaffar T, Arshad M, *et al*. Green synthesis of zinc ferrite nanoparticles for photocatalysis of methylene blue. International Journal of Phytoremediation. 2020;22(13):1440-1447. doi: https://doi.org/10.1080/15226514.2020.1781783

67. Bawazeer S. Green synthesis of silver nanoparticles from Euphorbia milii plant extract for enhanced antibacterial and enzyme inhibition effects. Int J of Health Sci. 2024;18(2):18-25. https://pubmed.ncbi.nlm.nih.gov/38455597/

68. Getie S, Belay A, Reddy AR C, Z B. Synthesis and Characterizations of Zinc Oxide Nanoparticles for Antibacterial Applications. J Nanomed Nanotechnol. 2017;s8(004):1-8. doi: https://doi.org/10.4172/2157-7439.s8-004

69. Raha S, Ahmaruzzaman M. ZnO nanostructured materials and their potential applications: progress, challenges and perspectives. Nanoscale Adv. 2022;4(8):1868-1925. doi: https://doi.org/10.1039/d1na00880c

70. Flores B, Guzman M, Chumpitaz O, Flores S, Rodriguez A, Herrera JE. Crystallographic and optical properties of ZnO nanoparticles prepared by two different methods. Appl. Phys. A. 2025;131(4):300. doi: https://doi.org/10.1007/s00339-025-08431-z

71. Kanimozhi S, Durga R, Sabithasree M, Kumar AV, Sofiavizhimalar A, Kadam AA, *et al*. Biogenic synthesis of silver nanoparticle using Cissus quadrangularis extract and its invitro study. Journal of King Saud University - Science. 2022;34(4):101930. doi: https://doi.org/10.1016/j.jksus.2022.101930

72. Gomathi M, Rajkumar P, Prakasam A, Ravichandran K. Green synthesis of silver nanoparticles using Datura stramonium leaf extract and assessment of their antibacterial activity. Resource-Efficient Technologies. 2017;3(3):280-284. doi: https://doi.org/10.1016/j.reffit.2016.12.005

73. Mallikarjuna K, John Sushma N, Narasimha G, Manoj L, Deva Prasad Raju B. Phytochemical fabrication and characterization of silver nanoparticles by using Pepper leaf broth. Arabian Journal of Chemistry. 2014;7(6):1099-1103. doi: https://doi.org/10.1016/j.arabjc.2012.04.001

74. Akpeji BH, Lari B, Igbuku UA, Tesi G, Elemike EE, Akusu PO. Synthesis and Characterization of MnO2 nanoparticles mediated by Raphia hookeri seed. J. Nig. Soc. Phys. Sci. 2024;6(4):2203. doi: https://doi.org/10.46481/jnsps.2024.2203

75. Akpeji BH, Bawa HA, Gbajabiamila AT, Elemike EE, Ogunsipe A, Amitaye AN, *et al*. Nanocomposites of Tin Hydroxide Phthalocyanine Sn(OH)2Pc and Titanium Dioxide Nanoparticles for Improved Antimicrobial Activities. J Inorg Organomet Polym. 2024;35(2):1292-1308. doi: https://doi.org/10.1007/s10904-024-03291-1

76. Ogwuche CE, Elemike EE, Oju D, Onwudiwe DC, Singh M, Akpeji BH. Synthesis, Characterization, Anticancer and Antimicrobial Potentials of Chrysothemis Pulchella Leaf Extract Mediated Gold Nanoparticles. J Inorg Organomet Polym. 2023;34(3):944-951. doi: https://doi.org/10.1007/s10904-023-02817-3

77. Sukarman, Kristiawan B, Khoirudin, Abdulah A, Enoki K, Wijayanta AT. Characterization of TiO2 nanoparticles for nanomaterial applications: Crystallite size, microstrain and phase analysis using multiple techniques. Nano-Structures & Nano-Objects. 2024;38(2):101168. doi: https://doi.org/10.1016/j.nanoso.2024.101168

78. Hassanzadeh-Tabrizi S. Precise calculation of crystallite size of nanomaterials: A review. Journal of Alloys and Compounds. 2023;968(40):171914. doi: https://doi.org/10.1016/j.jallcom.2023.171914

79. Crosera M, Bovenzi M, Maina G, Adami G, Zanette C, Florio C, *et al*. Nanoparticle dermal absorption and toxicity: a review of the literature. Int Arch Occup Environ Health. 2009;82(9):1043-1055. doi: https://doi.org/10.1007/s00420-009-0458-x

80. Ahmed KBA, Raman T, Veerappan A. Future prospects of antibacterial metal nanoparticles as enzyme inhibitor. Materials Science and Engineering: C. 2016;68(11):939-947. doi: https://doi.org/10.1016/j.msec.2016.06.034

81. Salleh A, Naomi R, Utami ND, Mohammad AW, Mahmoudi E, Mustafa N, *et al*. The Potential of Silver Nanoparticles for Antiviral and Antibacterial Applications: A Mechanism of Action. Nanomaterials. 2020;10(8):1566. doi: https://doi.org/10.3390/nano10081566

82. Happy Agarwal, Soumya Menon, Venkat Kumar S, Rajeshkumar S. Mechanistic study on antibacterial action of zinc oxide nanoparticles synthesized using green route. Chemico-Biological Interactions. 2018;286(8):60-70. doi: https://doi.org/10.1016/j.cbi.2018.03.008

83. Xiong P, Huang X, Ye N, Lu Q, Zhang G, Peng S, *et al*. Cytotoxicity of Metal-Based Nanoparticles: From Mechanisms and Methods of Evaluation to Pathological Manifestations. Advanced Science. 2022;9(16):2106049. doi: https://doi.org/10.1002/advs.202106049

Additional Information

How to Cite

APA 7th Edition: Onunkwo, I. C., Edema, M. O., Ogwuche, C. E. & Akpeji, B. H. (2026). Green-synthesized Zinc Oxide Nanoparticles from Cissus aralioides: Characterization, and Antimicrobial Potentials. Sciences of Phytochemistry, 5(1), 147-159. https://doi.org/10.58920/sciphy0501537

Vancouver: Onunkwo IC, Edema MO, Ogwuche CE, Akpeji BH. Green-synthesized Zinc Oxide Nanoparticles from Cissus aralioides: Characterization, and Antimicrobial Potentials. Sciences of Phytochemistry. 2026;5(1):147-159. https://doi.org/10.58920/sciphy0501537

Harvard: Onunkwo, I. C., Edema, M. O., Ogwuche, C. E. & Akpeji, B. H. (2026) 'Green-synthesized Zinc Oxide Nanoparticles from Cissus aralioides: Characterization, and Antimicrobial Potentials', Sciences of Phytochemistry, 5(1), pp. 147-159. doi: 10.58920/sciphy0501537

Publisher Note

Open Access